Supporting Information

Self-Assembly of Nanoparticles from Evaporating Sessile Droplets: Fresh Look into the Role of Particle/Substrate Interaction

N. Bridonneau,[1,2] M. Zhao,[1] N. Battaglini,[2] G. Mattana,[2] V. Thévenet,[1] V. Noël,[2] M. Roché,[1] S. Zrig[2*] and F. Carn[1*]

[1] Université de Paris, Laboratoire Matière et Systèmes Complexes, CNRS, UMR 7057, Paris, France.
[2] Université de Paris, ITODYS, CNRS, UMR 7086, 15 rue J-A de Baïf, F-75013 Paris, France

[*] E-mail : florent.carn@univ-paris-diderot.fr, samia.zrig@univ-paris-diderot.fr

1- Characterization of Nanoparticles and surfaces
- a. SEM-FEG images of SiNP(+) and SiNP(-) — Figure S1
- b. SEM-FEG images of AuNP(-) and UV-vis spectra of AuNP(citrates) and AuNPs(MUA) — Figure S2
- c. AFM and SEM-FEG images of Au, AuSub(+) and AuSub(-) — Figure S3

2- Contact angle measurements
- a. Contact angles of SiNPs(-) and SiNP(+) (data) — Table S1
- b. Contact angles of SiNPs(-) (pictures) — Table S2
- c. Contact angles of SiNPs(+) (pictures) — Table S3
- d. Contact angles of AuNPs(-) — Table S4
- e. Contact angles of AuNPs(-) (pictures) — Table S5
- f. Contact angles measurements — Figure S4

3- Width of the coffee-ring
- a. For SiNPs(-) and SiNP(+) — Table S6
- b. For AuNPs(-) — Table S7
- c. Coffee-ring width for SiNP(+), SiNP(-) and AuNPs(-) — Figure S5
- d. Coffee-ring width in respect to the drop size — Figure S6

4- Profilometry measurements
- a. For SiNPs(+) — Table S8
- b. For SiNPs(-) — Table S9
- c. For AuNPs(-) — Table S10

5- Evolution of the drop diameter
- a. Drop diameter in respect to the deposited volume — Table S11
- b. Drop diameter in respect to the deposition height — Table S12

6- Deposition of SiNP(+) on AuSub(+) surface

a. Increase of the central spot size Figure S7
b. Patterns observed at different magnifications Figure S8
c. Repeatability measurements Figure S9
d. Effect of salt addition to SiNP(+) patterns Figure S10

7- Deposition of SiNP(+) on AuSub(+), AuSub(-) and Au surfaces

a. From 0.1 to 100g/L Figure S11

8- Deposition of SiNP(-) on positive(+) surface

a. From 0.001 to 100g/L Figure S12
b. Effect of salt addition Figure S13
c. Example of visible cracks Figure S14

9- Deposition of AuNP(-) on positive(+) and negative(-) surfaces

a. Increasing concentration from [stock]/100 to [stock] Figure S15
b. Effect of salt addition on the deposited patterns Figure S16

1- Characterization of nanoparticles and surfaces

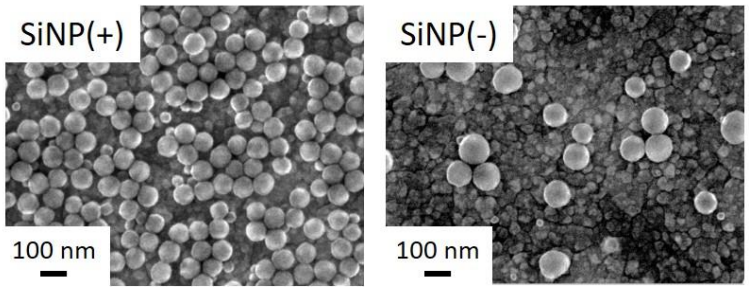

Figure S1. SEM-FEG images of SiNP(+) and SiNP(-).

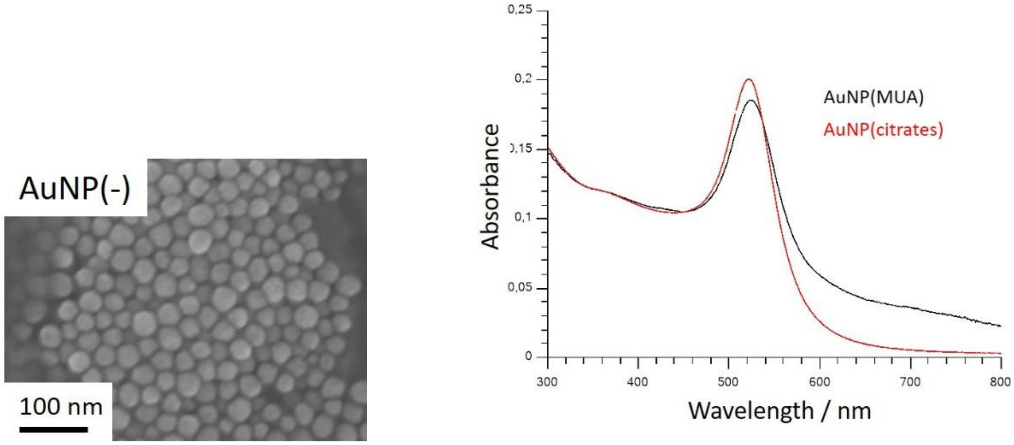

Figure S2. SEM-FEG images of AuNP(-) nanoparticles and UV-vis spectra of AuNP(citrates) and AuNPs(MUA) (named AuNP(-)) solutions.

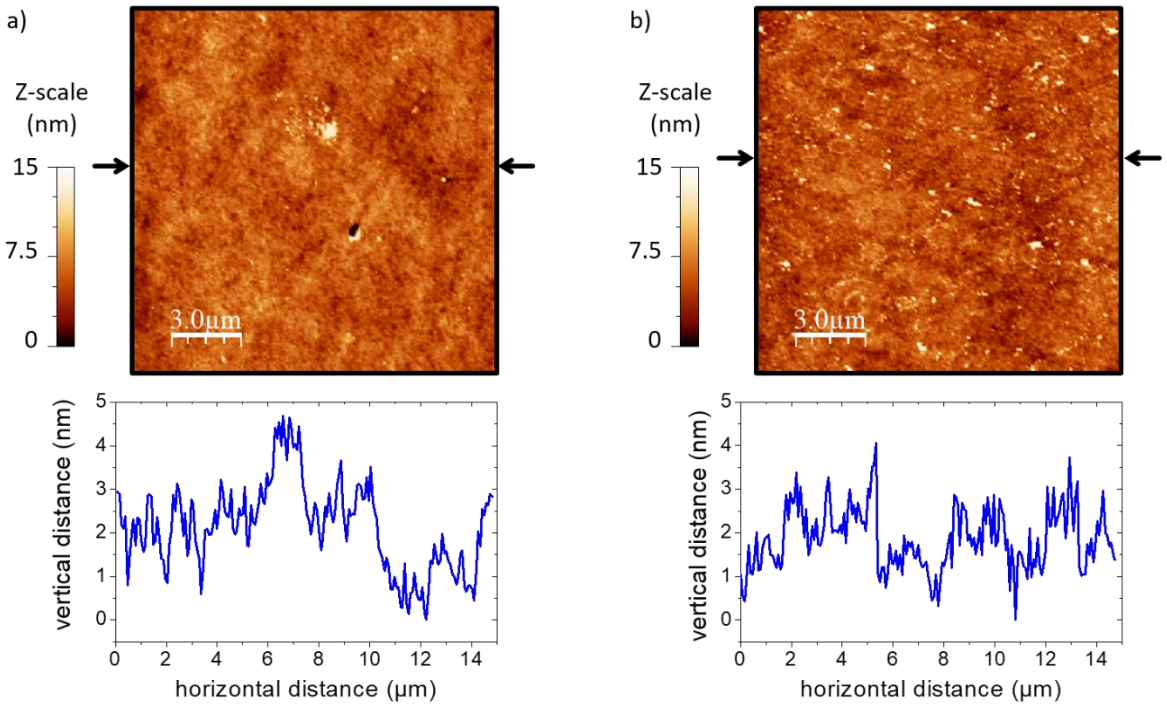

Figure S3. a-b) AFM images (15x15µm^2) and line profiles of bare Au surface and AuSub(+) surface, respectively. The arrows on the borders of the images indicate the position of the cross sections.

2- Contact angle measurements

SiNP(-)									
concentration (g/L)	0.01	0.02	0.03	0.05	0.1	0.5	0.7	1	0.05 + NaCl 25mM
Au	-	84.9 ± 1.84	87.6 ± 2.14	95.0	48.5	-	83.4 ± 0.88	103.1 ± 3.44	105.7 ± 2.11
AuSub(+)	59.7	57.7	64.9	75.3	61.5 ± 0.58	63.3	66.4 ± 2.28	54.4 ± 0.75	64.1 ± 1.15
AuSub(-)	54.5	51.7	59.5 ± 0.87	58.8 ± 0.97	52.3 ± 2.39	57.5	52.4 ± 1.58	55.5 ± 5.64	56.5 ± 1.84

SiNP(+)									
concentration (g/L)	0.01	0.02	0.03	0.05	0.1	0.5	0.7	1	0.05 + NaCl 50mM
Au	71.3 ± 1.86	75.8 ± 1.75	86.8 ± 1.93	77.0 ± 3.28	76.2 ± 2.53	81.7 ± 4.87	77.6 ± 0.99	79.5 ± 0.62	79.5 ± 0.65
AuSub(+)	70.7 ± 11.87	59.4 ± 4.52	55.5 ± 1.79	65.7 ± 9.17	57.2 ± 1.61	58.7 ± 1.39	58.2 ± 1.74	61.5 ± 3.46	54.4 ± 11.59
AuSub(-)	58.0 ± 2.45	59.1 ± 2.18	63.0 ± 4.72	55.9 ± 2.34	61.6 ± 1.00	57.8 ± 1.80	61.2 ± 0.81	60.1 ± 1.19	56.7 ± 2.93

Table S1. Contact angles of SiNPs(-) and SiNP(+).

SiNP(-)					
concentration (g/L)	0.01	0.02	0.03	0.05	0.1
Au	-	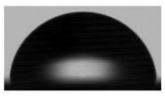	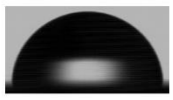	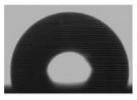	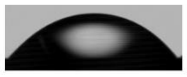
AuSub(+)	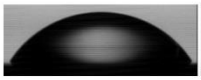		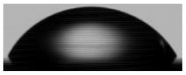	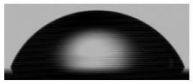	
AuSub(-)	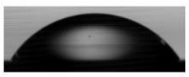		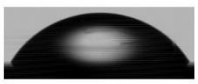	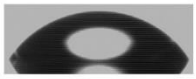	

Concentration (g/L)	0.5	0.7	1	0.05 + NaCl 25mM
Au	-	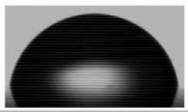	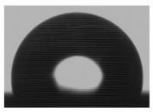	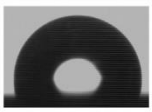
AuSub(+)	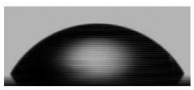	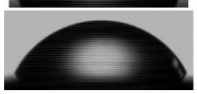	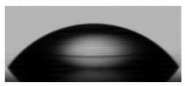	
AuSub(-)	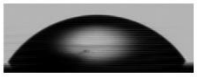	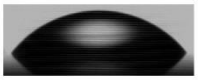	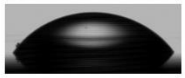	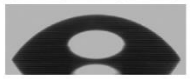

Table S2. Contact angles of SiNPs(-) (pictures).

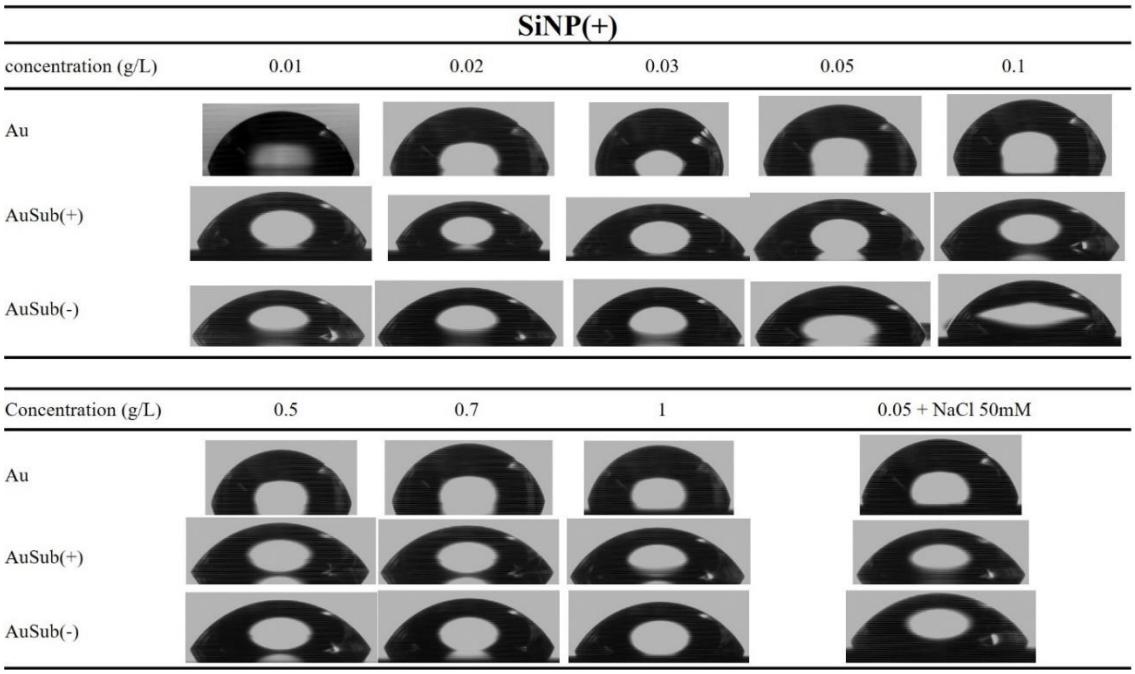

Table S3. Contact angles of SiNPs(+) (pictures).

AuNP(MUA-)									
concentration	c/100	c/80	c/40	c/20	c/10	c/6	c/4	c/2	c
Au	-	79.0	88.1	84.4	77.4	72.1	70.3	75.4	72.2
AuSub(+)	56.1	55.3	58.5	59.0	49.6	54.1	50.4	52.2	44.8
AuSub(-)	52.8	56.3	65.9	62.2	61.8	56.7	53.8	47.6	48.3

Table S4. Contact angles of AuNPs(-).

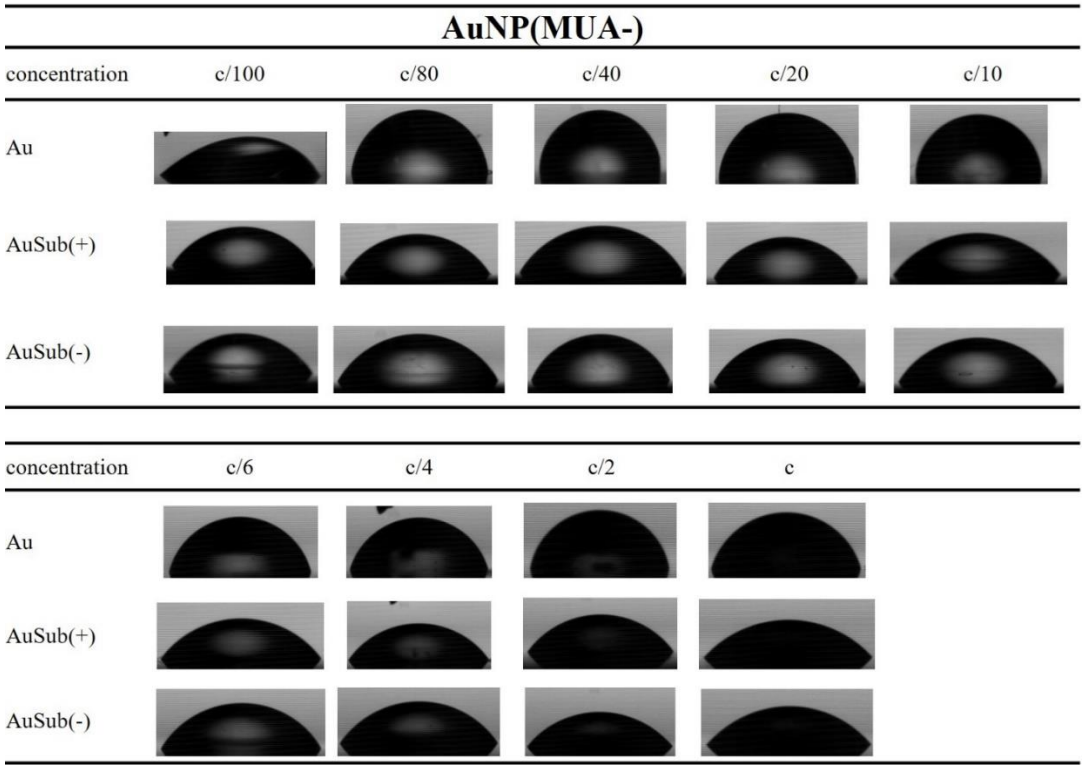

Table S5. Contact angles of AuNPs(-) (pictures).

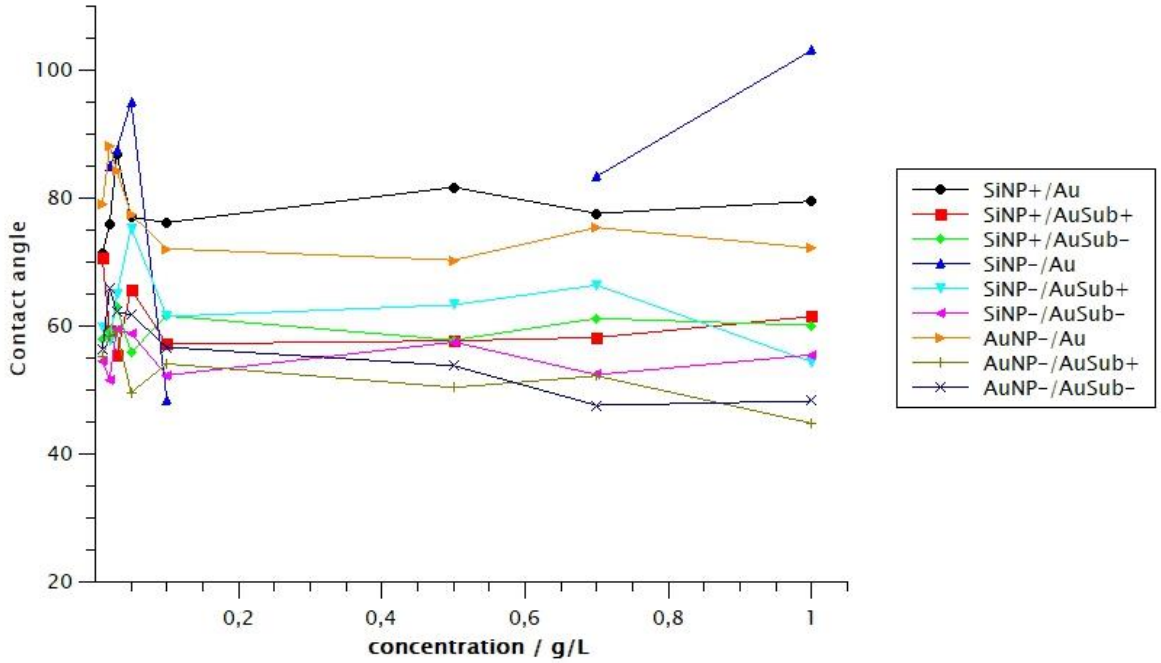

Figure S4. Contact angle measurements for SiNP+, SiNP- and AuNP- deposited on AuSub, AuSub+ and AuSub-.

3- Size of the coffee-ring

SiNP(+)									
concentration	0.01	0.02	0.03	0.05	0.1	0.3	0.5	0.7	1
AuSub(+)	1.5	1.8	3.3	3.9	0.3	1.7	11	15.0	19.2
AuSub(-)	2.8	2.1	2.3	2.1	1.8	6.0	12.3	14.9	20.8
Au	-	-	-	-	-	3.2	5.7	15.4	17.5

SiNP(-)									
AuSub(+)	3.3	6.3	9.7	14.6	8.9	23.4	25.6	31.1	42.7
AuSub(-)	3.8	6.5	9.6	11.6	9.2	19.6	30.9	25.8	35.2
Au		7.1	9.6	14.2	9.9	12.7	19.7	10.0	

Table S6. coffee-ring sizes for SiNPs(-) and SiNP(+) (µm).

AuNP(-)									
concentration	c	c/2	c/4	c/6	c/8	c/10	c/20	c/40	c/100
AuSub(+)	14.5	12.5	10.6	9.6	8.9	7.6	6.2	4.3	2.8
AuSub(-)		12.9	10.6	8.3	8.1	7.0	6.4	4.95	2.5

Table S7. coffee-ring sizes for AuNPs(-) (µm).

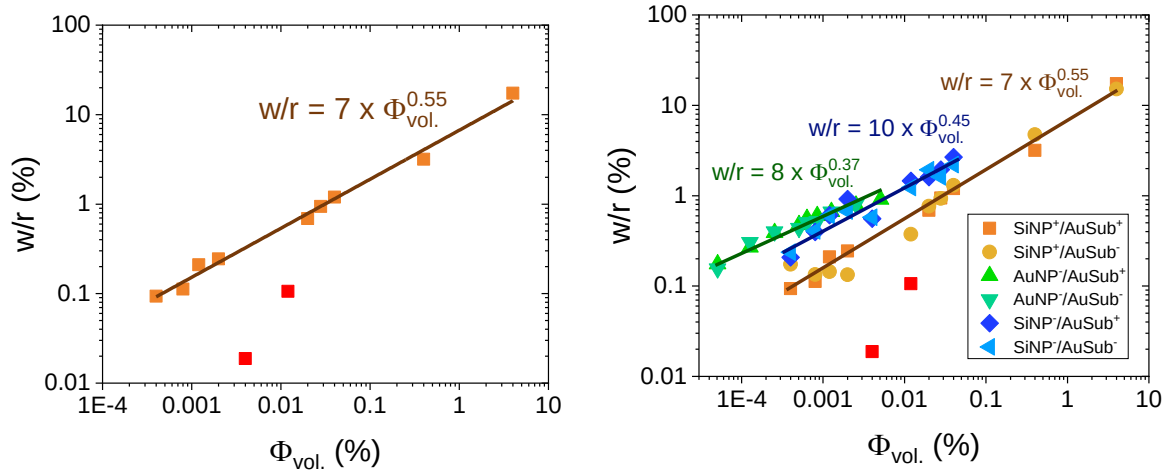

Figure S5. coffee-ring width for SiNP(+), SiNP(-) and AuNPs(-) on surfaces AuSub(+) and AuSub(-).

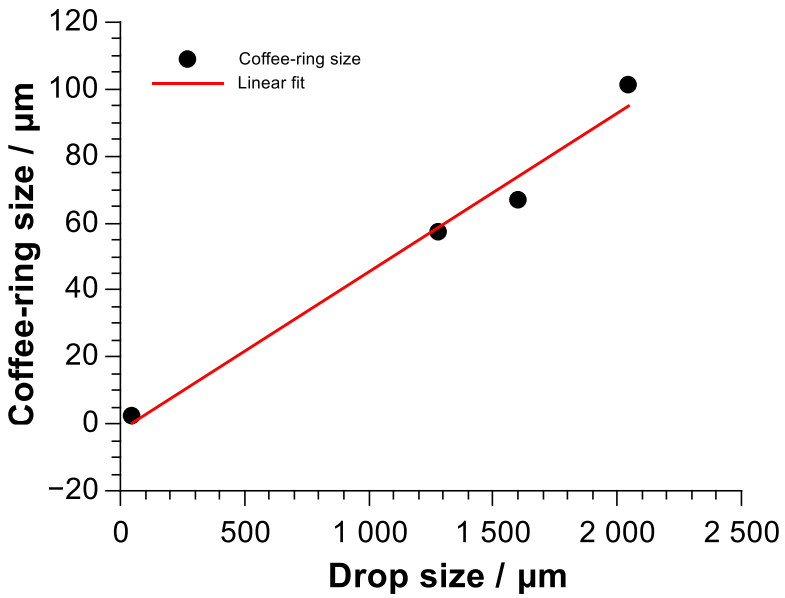

Figure S6. coffee-ring width in respect to the drop size (R^2 = 0.98) for SiNP(+) on surface AuSub(+).

4- Profilometry measurements

	SiNP(+)	
	Low concentrations	High concentrations
Au	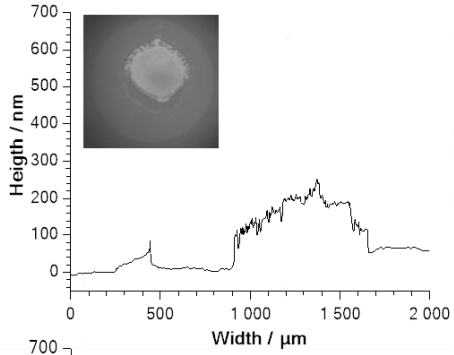	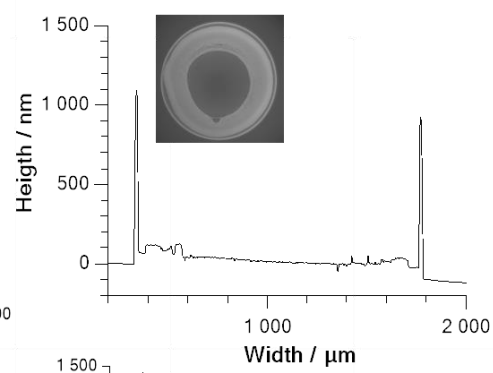
AuSub(-)	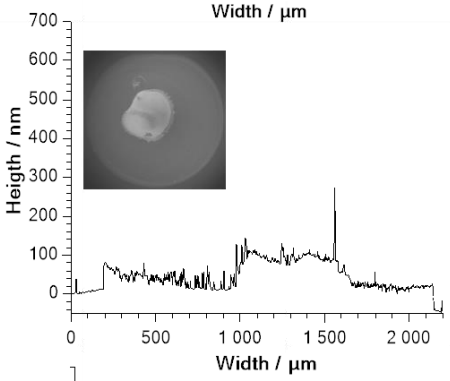	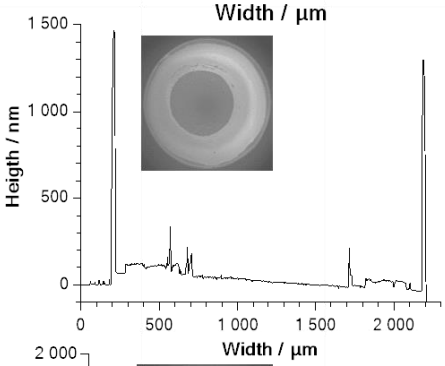
AuSub(+)	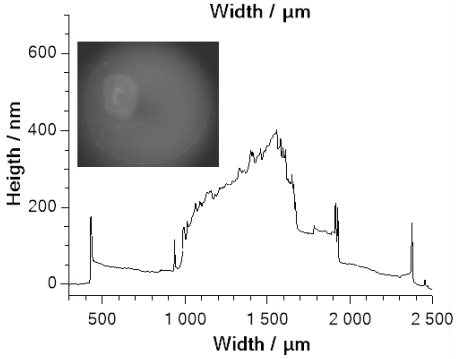	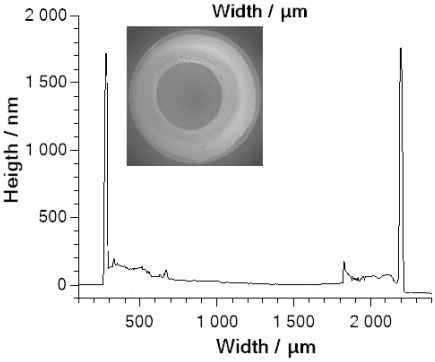

Table S8. Profilometry measurements for SiNPs(+).

SiNP(-)		
	Low concentrations	High concentrations
AuSub(-)	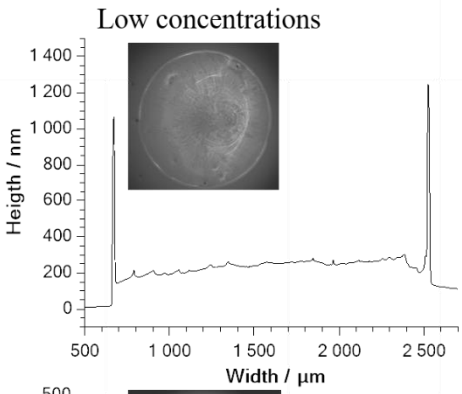	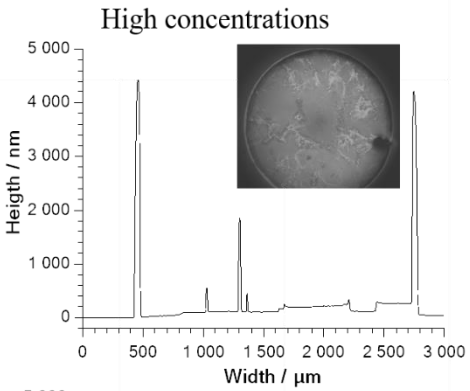
AuSub(+)	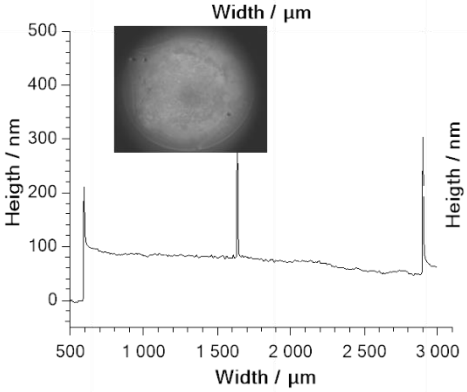	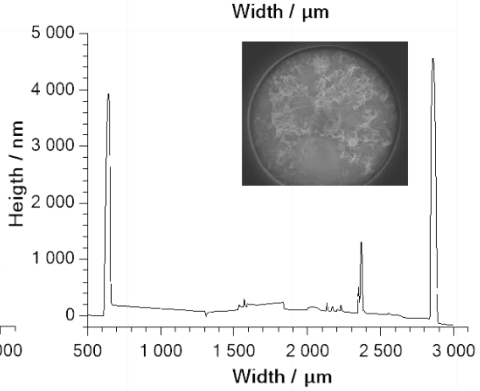

Table S9. Profilometry measurements for SiNPs(-).

AuNP(-)		
	Low concentrations	High concentrations
AuSub(-)	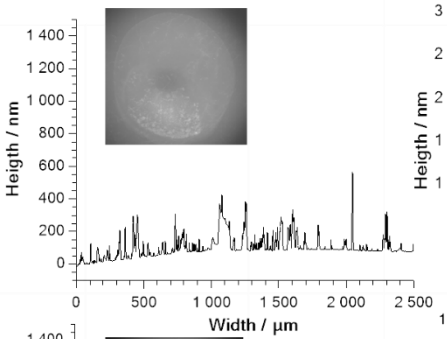	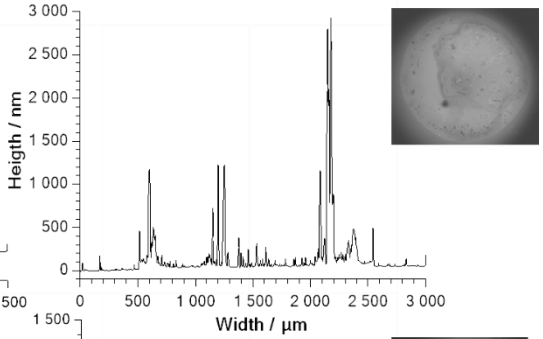
AuSub(+)	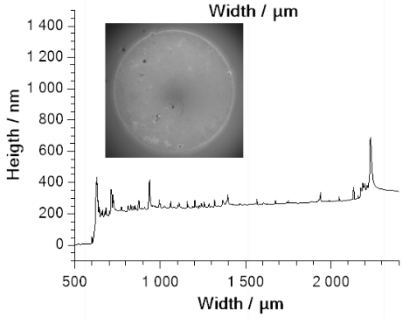	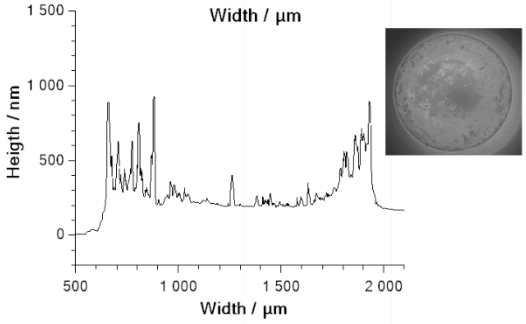

Table S10. Profilometry measurements for AuNPs(-).

5- Evolution of the drop diameter

Drop volume / µL	0.05	0.1	0.2	1
Drop diameter / mm	2.065	2.220	2.057	2.462

Table S11. Evolution of the drop diameter in respect to the deposited volume for SiNP(+) on AuSub(+).

Height / cm	0	0.5	1	2	3
Drop diameter / mm	1.752	3.1	3.35	3.66	3.26

Table S12. Drop diameter in respect to the deposition height.

6- Deposition of SiNP(+) on AuSub(+) surface

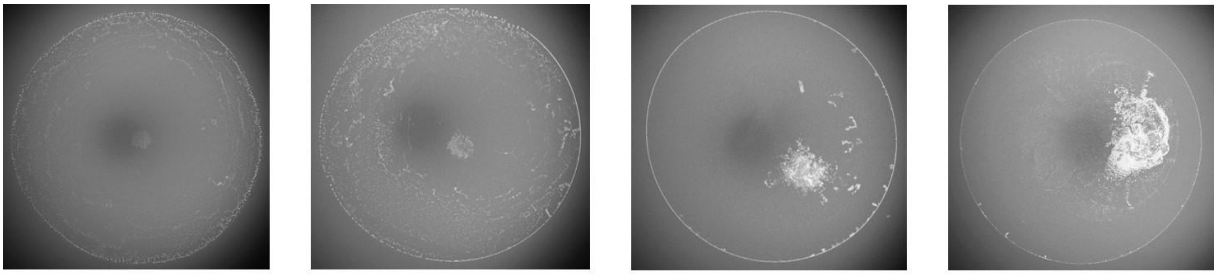

0.02 g/L
104 µm

0.03 g/L
148 µm

0.04 g/L
258 µm

0.1 g/L
318 µm

Figure S7. Increase of the central dot size at low concentration, for SiNP(+) on AuSub(+).

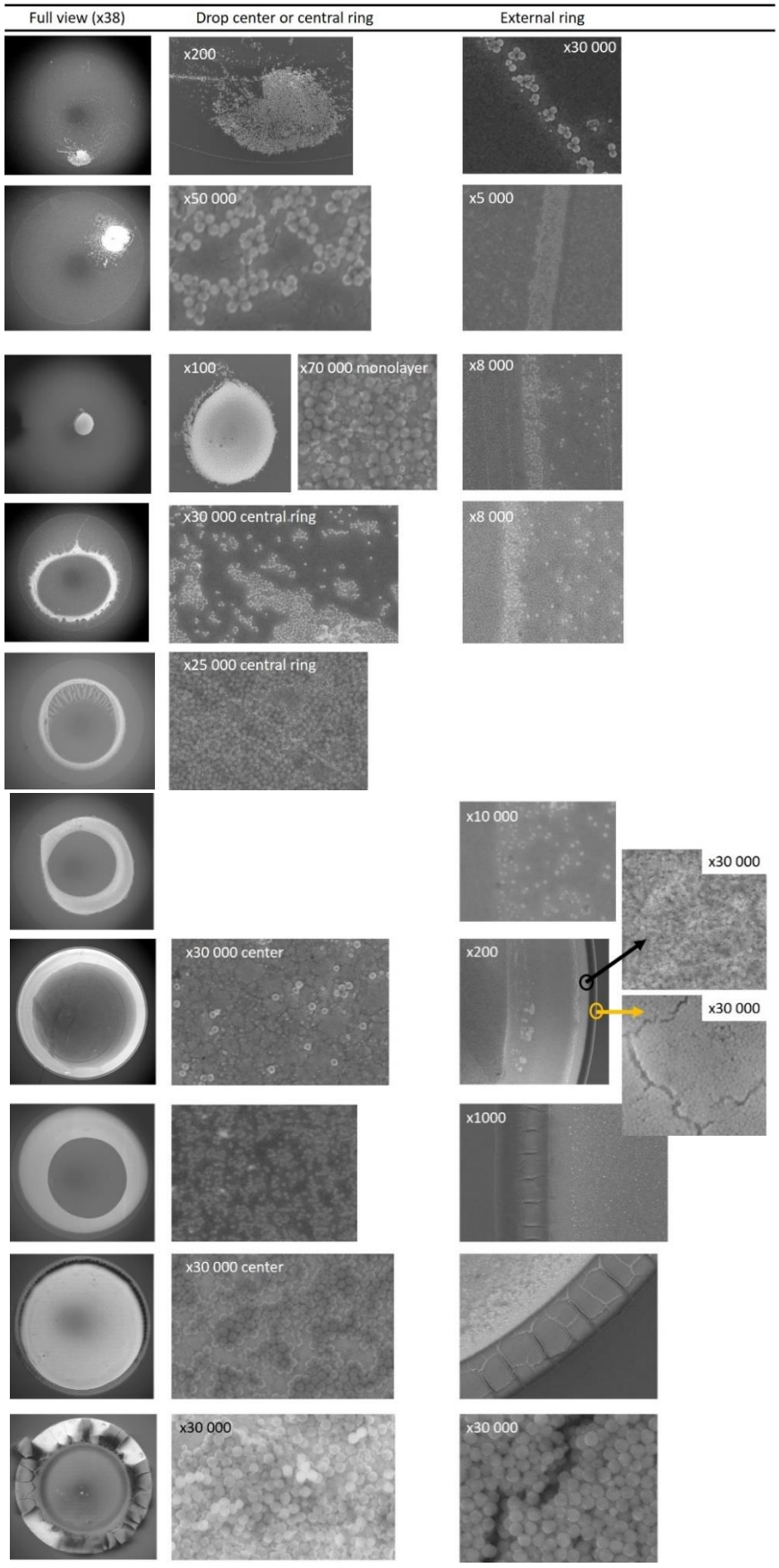

Figure S8. Patterns observed at different magnifications, increasing the concentration from top for SiNP(+) on AuSub(+).

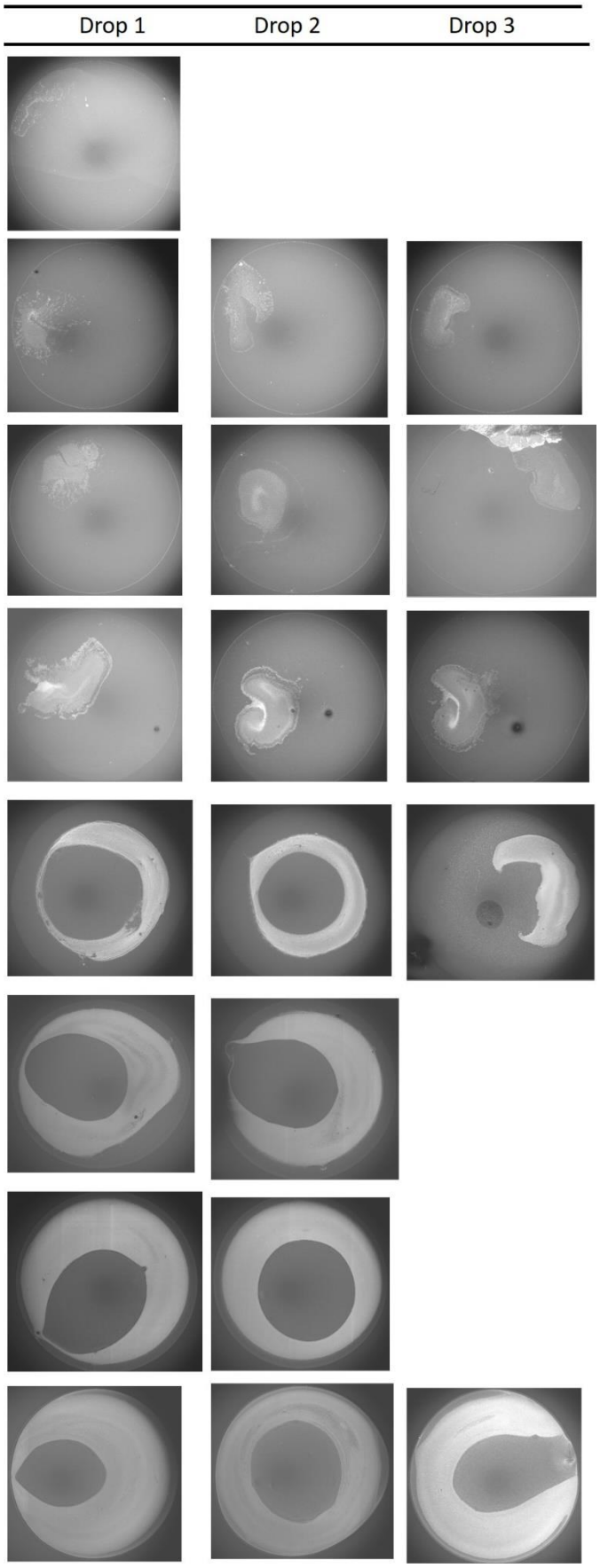

Figure S9. Repeatability measurements, increasing the concentration from top to bottom for SiNP(+) on AuSub(+).

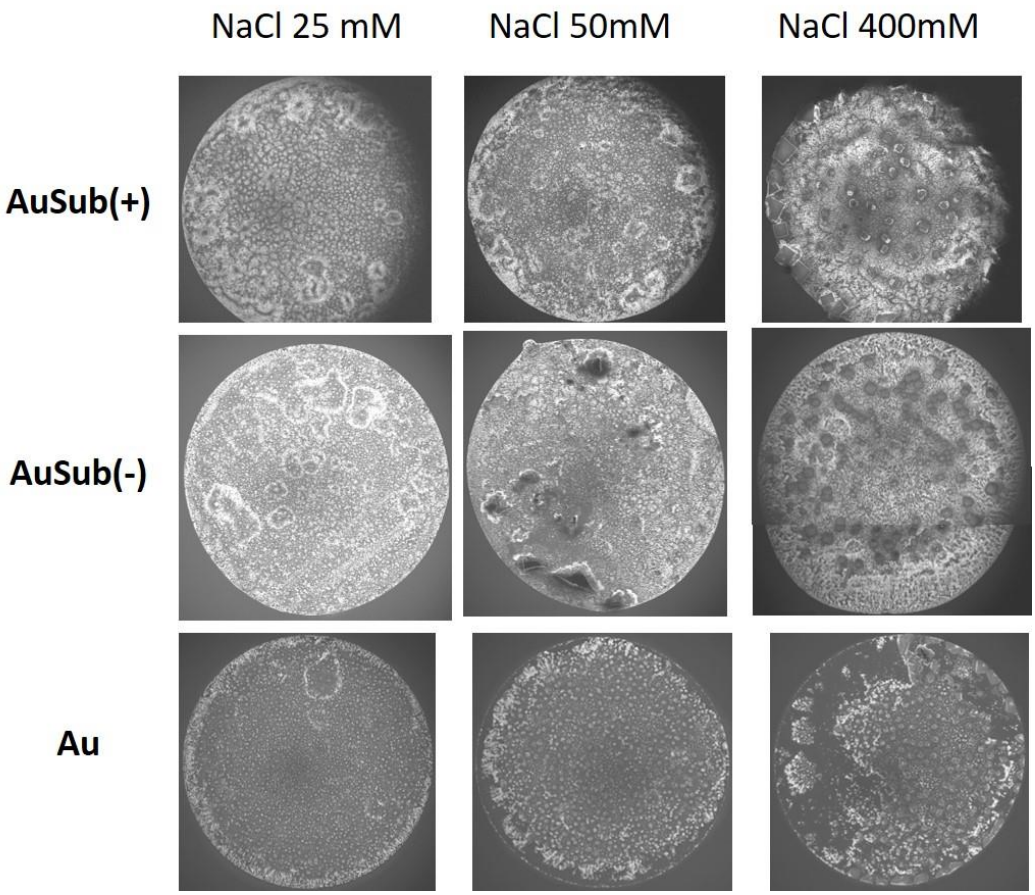

Figure S10. The effect of salt addition to SiNP(+) solutions.

7- Deposition of SiNP(+) on AuSub(+), AuSub(-) and Au surfaces

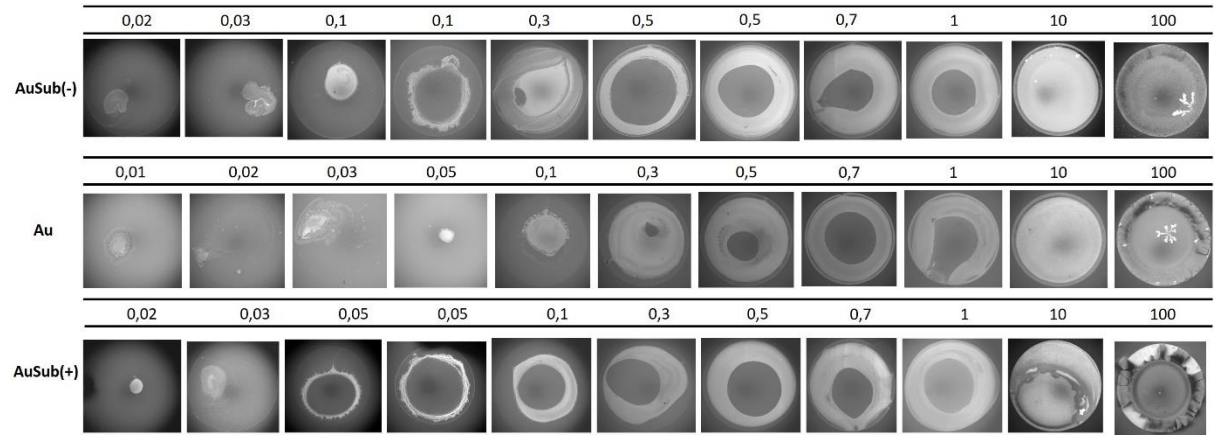

Figure S11. Dry patterns of SiNP(+) on positive, negative and bare Au surfaces.

8- Deposition of SiNP(-) on AuSub(+) surface

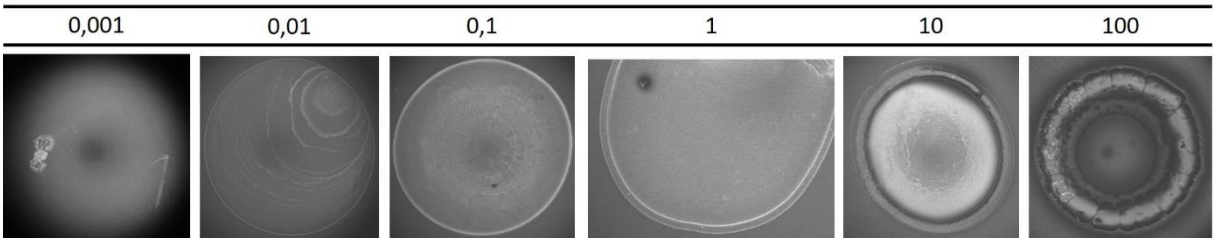

Figure S12. Deposition of SiNP(-) on positive(+) surface.

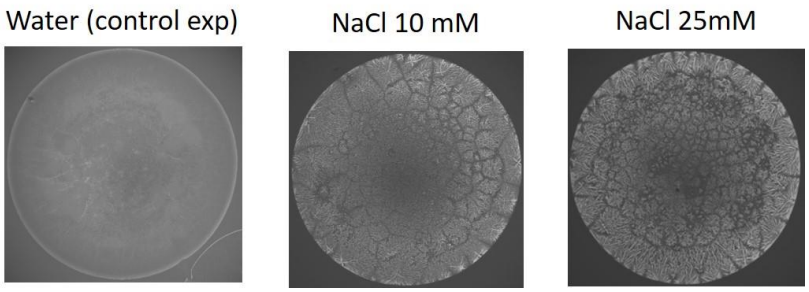

Figure S13. effect of salt addition on AuSub(+) surface at 0.1 g/L.

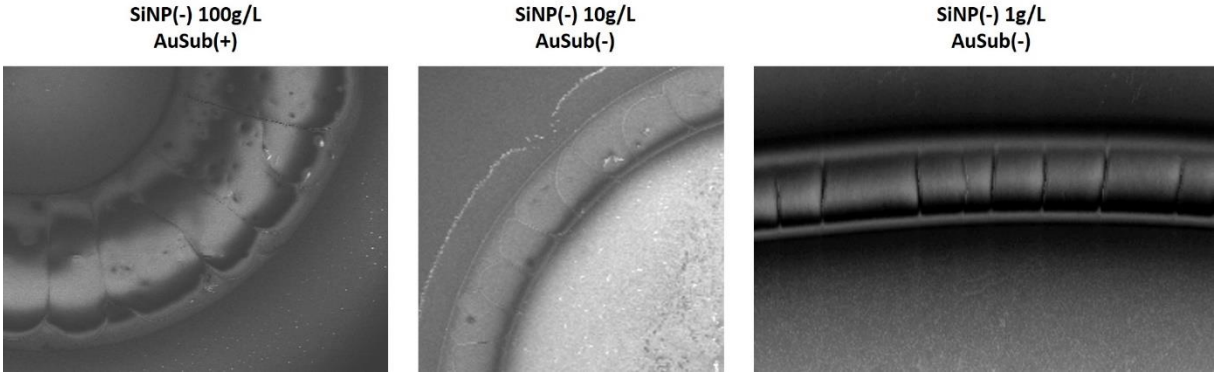

Figure S14. Examples of visible cracks observed on the external particle ring.

9- Deposition of AuNP(-) on AuSub(+) and AuSub(-) surfaces

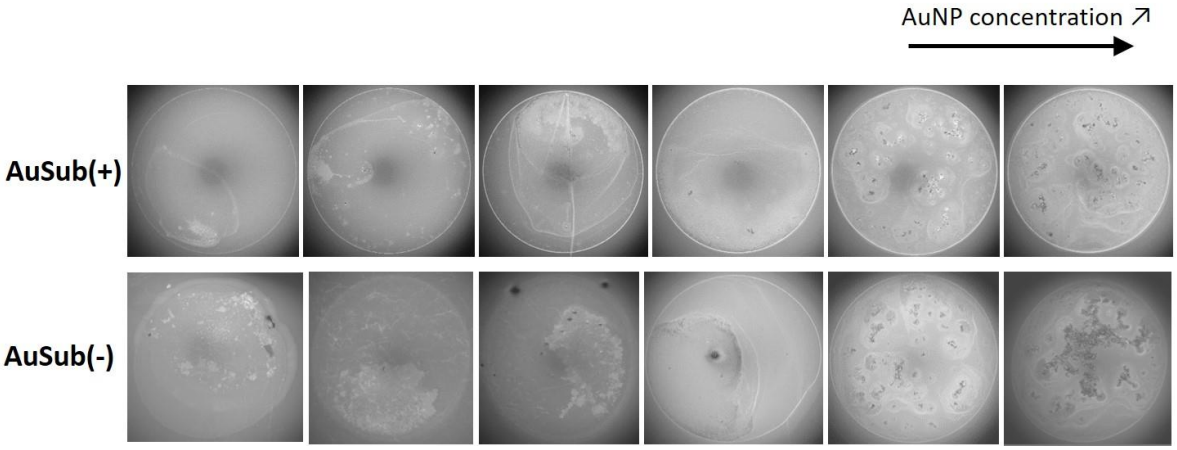

Figure S15. Deposition of AuNP(-) on positive(+) and negative(-) surfaces, increasing concentration from [stock]/100 to [stock].

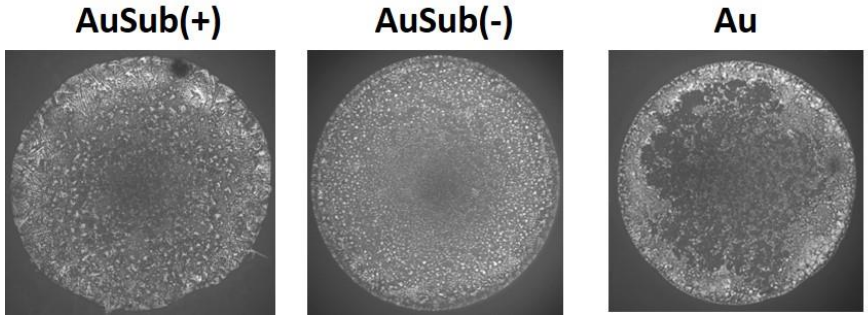

Figure S16. Effect of salt addition (25 mM) on the deposited patterns.

10. Calculation of the DLVO interaction potential between a nanoparticle and the substrate.

NP	R nm	$\Psi_{P.}$ mV	Sub	$\Psi_{S.}$ mV	$W_{El.}$ kT	$W_{vdW.}$ kT	W_{DLVO} kT	Θ °
SiNP^{+}	37.5	+ 50	**AuSub^{+}**	+ 140	3.3×10^{2}	$-4\times10^{-9}/-2\times10^{-6}$	3.3×10^{2}	60
			AuSub^{bare}	- 15	-54	$-4\times10^{-9}/-2\times10^{-6}$	-54	78
			AuSub^{--}	- 140	-3.3×10^{2}	$-4\times10^{-9}/-2\times10^{-6}$	-3.3×10^{2}	59
SiNP^{-}	45.0	- 50	**AuSub^{+}**	+ 140	-4×10^{2}	$-6\times10^{-9}/-2\times10^{-6}$	-4×10^{2}	52
			AuSub^{--}	- 140	4×10^{2}	$-6\times10^{-9}/-2\times10^{-6}$	4×10^{2}	53
AuNP^{-}	15.0	- 37	**AuSub^{+}**	+ 140	-10^{2}	$-1\times10^{-9}/-1\times10^{-6}$	-10^{2}	52
			AuSub^{--}	- 140	10^{2}	$-1\times10^{-9}/-1\times10^{-6}$	10^{2}	53

Table S13. Nanoparticles (NP) and Substrates (Sub) used in this study with their acronym and main characteristics: particle radius measured by SEM-FEG (R, see figure S1 and S2), particle surface potential ($\Psi_{P.}$) assumed to be equal to the zeta potential knowing that this is an underestimation, substrate surface potential ($\Psi_{S.}$), Hamaker constant Particle/Water/Gold ($H_{in\ water}$), electrostatic double layer energy ($W_{El.}$), van der Waals energy ($W_{vdW.}$), DLVO energy (W_{DLVO}) and equilibrium contact angle averaged on the different concentrations (Θ, see Table S1-S5 and Figure S4). We indicate the minimum/maximum forces that have been calculated before drying (t_0) for $D = \kappa^{-1}$ at the initial minimum/maximum particle concentrations respectively. The evolution of κ^{-1} and W_{DLVO} with the initial particle concentration is plotted in the Figure 1. Negative energy implies attraction.

11. Hamaker constant determination.

The non retarded Hamaker constants (H) used for the van der Waals force calculations were determined as follows. We used a gold/water/gold Hamaker constant of 2.5×10^{-19} J corresponding to the value determined experimentally by S. Biggs & P. Mulvaney,[1] and theoretically by Y.I. Rabinovich and N.V. Churaev using the Lifschitz theory.[2]

We did not directly find the value of the silica/water/gold Hamaker constant. On the other hand, we found several values for the silica/water/silica Hamaker constant : 1.5×10^{-20} J,[3] 0.22×10^{-20} J,[4] and 0.24×10^{-20} J.[5] We decided to take an average of these values and estimate the silica/water/gold Hamaker constant by the using the following expression:[6]

$$H_{\text{silica/water/gold}} \approx \sqrt{H_{\text{silica/water/silica}} * H_{\text{gold/water/gold}}}$$

$$\approx 4.3 \times 10^{-20}\, J$$

We underline that the approximate character of $H_{\text{silica/water/gold}}$ should not have a significant impact on the estimate of F_{DLVO}, given that $F_{vdW} << F_{El.}$ in all cases.

12. Laser Doppler velocimetry measurements.

a)

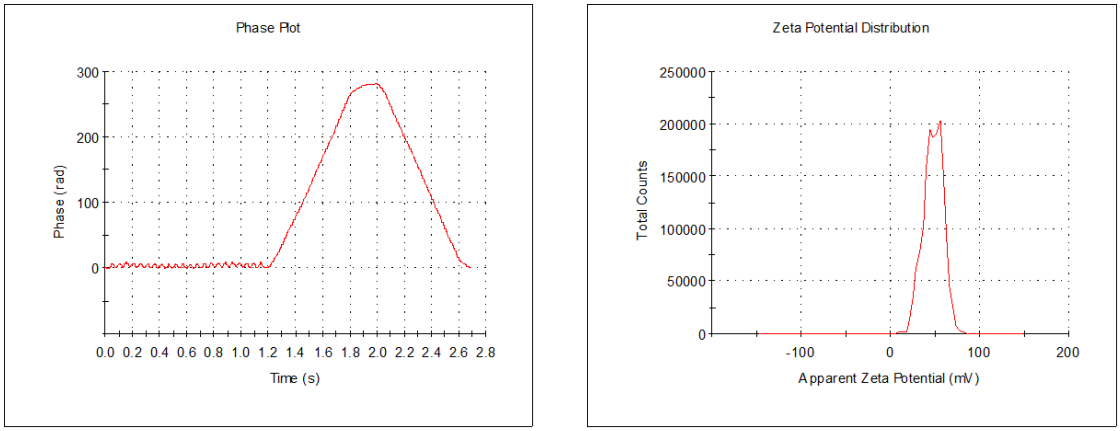

b)

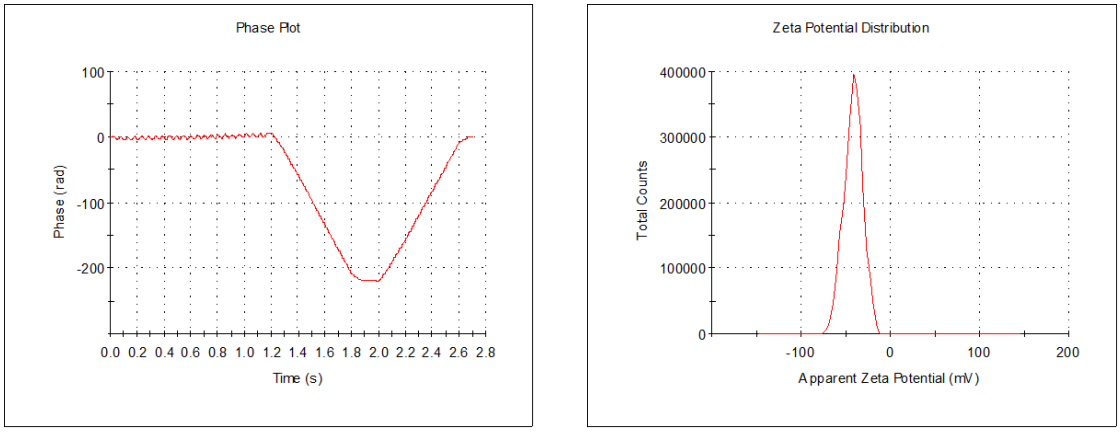

c)

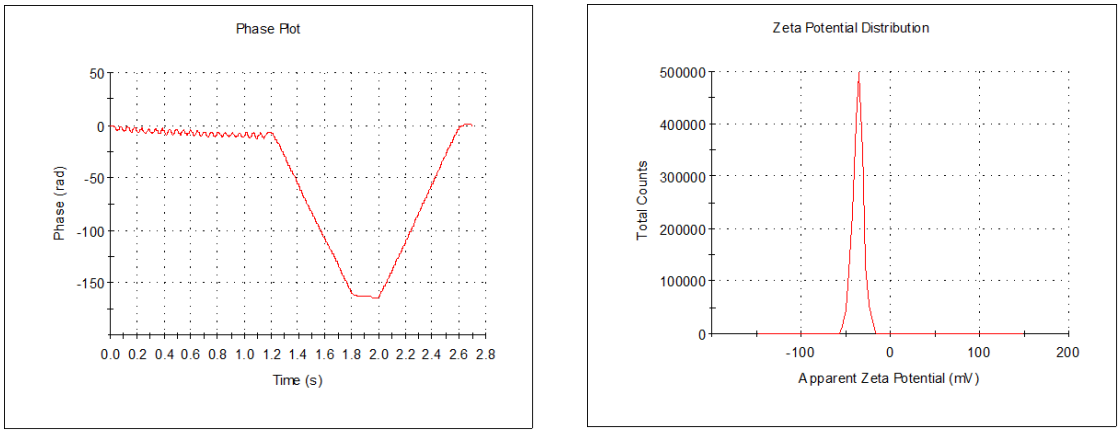

Figure S17. Typical Laser Doppler velocimetry characterizations of (a) $SiNP^{+}$, (b) $SiNP^{-}$ and (c) $AuNP^{-}$. Phase plot appear on the on the left and Zeta potential distribution on the right.

13. Focus on dot like patterns observed in the dilute regime for different NP/substrate combinations.

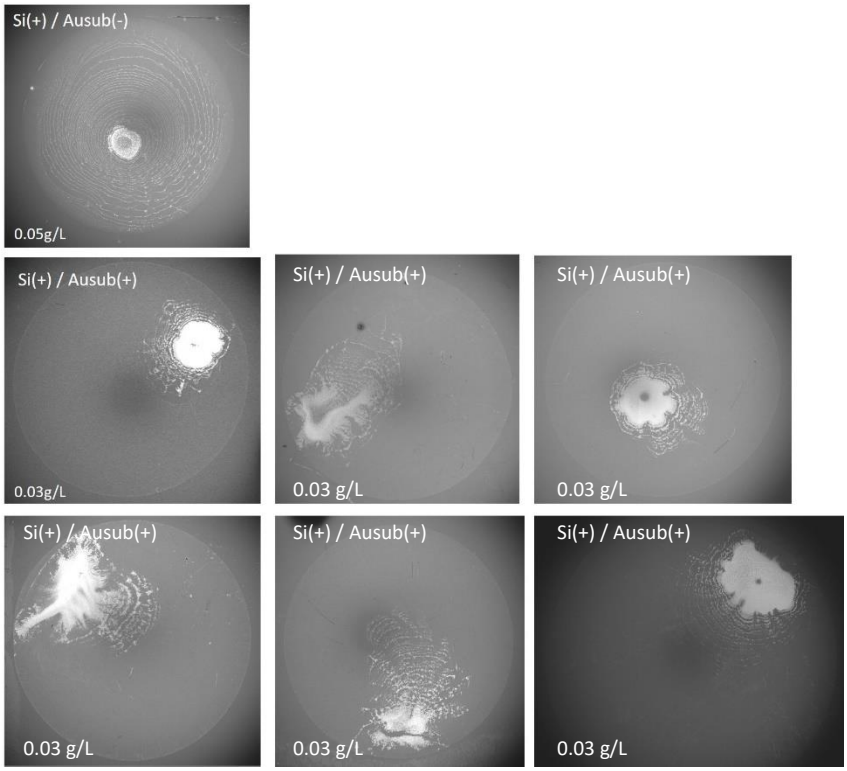

Figure S18. Deposition of SiNP(+) on positive(+) and negative(-) surfaces in the dilute range of concentration.

References.

(1) Biggs, S.; Mulvaney, P. Measurement of the Forces between Gold Surfaces in Water by Atomic Force Microscopy. *The Journal of Chemical Physics* **1994**, *100* (11), 8501–8505. https://doi.org/10.1063/1.466748.

(2) RABINOVICH, Y. I.; Churaev, N. V. RESULTS OF NUMERICAL-CALCULATIONS OF DISPERSION FORCES FOR SOLIDS, LIQUID INTERLAYERS, AND FILMS. *COLLOID JOURNAL OF THE USSR*. 1990, pp 256–262.

(3) Fielden, M. L.; Hayes, R. A.; Ralston, J. Oscillatory and Ion-Correlation Forces Observed in Direct Force Measurements between Silica Surfaces in Concentrated CaCl2 Solutions. *Physical Chemistry Chemical Physics* **2000**, *2* (11), 2623–2628. https://doi.org/10.1039/b001672l.

(4) Dishon, M.; Zohar, O.; Sivan, U. From Repulsion to Attraction and Back to Repulsion: The Effect of NaCl, KCl, and CsCl on the Force between Silica Surfaces in Aqueous Solution. *Langmuir* **2009**, *25* (5), 2831–2836. https://doi.org/10.1021/la803022b.

(5) Valmacco, V.; Elzbieciak-Wodka, M.; Besnard, C.; Maroni, P.; Trefalt, G.; Borkovec, M. Dispersion Forces Acting between Silica Particles across Water: Influence of Nanoscale Roughness. *Nanoscale Horizons* **2016**, *1* (4), 325–330. https://doi.org/10.1039/C6NH00070C.

(6) Israelachvili, J. N. *Intermolecular and Surface Forces*, Third edition.; Elsevier, Academic Press: Amsterdam, 2011.